The Astrophysical Journal, 857:58 (8pp), 2018 April 10 https://doi.org/10.3847/1538-4357/aab6b6

Can a Bright and Energetic X-Ray Pulsar Be Hiding Amid the Debris of SN 1987A?

Paolo Esposito[1], Nanda Rea[1,2,3], Davide Lazzati[4], Mikako Matsuura[5], Rosalba Perna[6], and José A. Pons[7]
[1] Anton Pannekoek Institute for Astronomy, University of Amsterdam, Postbus 94249, 1090 GE Amsterdam, The Netherlands; P.Esposito@uva.nl
[2] Institute of Space Sciences (IEEC–CSIC), Campus UAB, Carrer de Can Magrans s/n, E-08193 Barcelona, Spain
[3] Institut d'Estudis Espacials de Catalunya (IEEC), Gran Capità 2-4, 08034, Barcelona, Spain
[4] Department of Physics, Oregon State University, 301 Weniger Hall, Corvallis, OR 97331, USA
[5] School of Physics and Astronomy, Cardiff University, Queens Buildings, The Parade, Cardiff, CF24 3AA, UK
[6] Department of Physics and Astronomy, Stony Brook University, Stony Brook, NY 11794, USA
[7] Department de Física Aplicada, Universitat d'Alacant, Ap. Correus 99, E-03080 Alacant, Spain
Received 2017 August 2; revised 2018 March 10; accepted 2018 March 12; published 2018 April 13

Abstract

The mass of the stellar precursor of supernova (SN) 1987A and the burst of neutrinos observed at the moment of the explosion are consistent with the core-collapse formation of a neutron star. However, no compelling evidence for the presence of a compact object of any kind in SN 1987A has been found yet in any band of the electromagnetic spectrum, prompting questions on whether the neutron star survived and, if it did, on its properties. Beginning with an analysis of recent *Chandra* observations, here we appraise the current observational situation. We derived limits on the X-ray luminosity of a compact object with a nonthermal, Crab-pulsar-like spectrum of the order of $\approx(1\text{–}5)\times10^{35}$ erg s^{-1}, corresponding to limits on the rotational energy loss of a possible X-ray pulsar in SN 1987A of $\approx(0.5\text{–}1.5)\times10^{38}$ erg s^{-1}. However, a much brighter X-ray source cannot be excluded if, as is likely, it is enshrouded in a cloud of absorbing matter with a metallicity similar to that expected in the outer layers of a massive star toward the end of its life. We found that other limits obtained from various arguments and observations in other energy ranges either are unbinding or allow a similar maximum luminosity of the order of $\approx10^{35}$ erg s^{-1}. We conclude that while a pulsar alike the one in the Crab Nebula in both luminosity and spectrum is hardly compatible with the observations, there is ample space for an "ordinary" X-ray-emitting young neutron star, born with normal initial spin period, temperature, and magnetic field, to be hiding inside the evolving remnant of SN 1987A.

Key words: stars: neutron – supernovae: individual (SN 1987A)

1. Introduction

The supernova (SN) designated "1987A" was discovered on 1987 February 23 in the Large Magellanic Cloud (LMC). It was the brightest and nearest SN explosion observed since Kepler's SN 1604 and is providing a wealth of information on the last evolutionary stage of massive stars as well as on the formation of a supernova remnant (Arnett et al. 1989; McCray 1993; McCray & Fransson 2016). The explosion also confirmed the collapse of the progenitor star's core in SNe II through a burst of neutrinos detected by multiple instruments (Alekseev et al. 1987; Bionta et al. 1987; Hirata et al. 1987).

SN 1987A is surrounded by a triple-ring system that formed ∼20 kyr before the explosion from material ejected by the progenitor, possibly as a result of its fast rotation or a binary merger (Morris & Podsiadlowski 2007; Chita et al. 2008). The progenitor was identified in pre-explosions images to be Sanduleak (Sk) −69° 202, which was a B3 I blue supergiant with mass estimated at $\sim14\,M_{\odot}$ at the time of the explosion and initially at $\sim20\,M_{\odot}$, while in the case of a binary merger, the standard model assumes two stars originally of ∼15 and $\sim5\,M_{\odot}$ (Rousseau et al. 1978; Gilmozzi et al. 1987; Hillebrandt et al. 1987; Sonneborn et al. 1987; Woosley et al. 1987; Walborn et al. 1989; Podsiadlowski 1992).

The progenitor's mass and the neutrino flash observed at the time of the SN are consistent with the birth of a neutron star, though the formation of a black hole, directly or at a later time from fallback, cannot be excluded (Perego et al. 2015; Blum & Kushnir 2016). So far, however, no convincing detection of a neutron star—such as the observation of pulsed emission or of a point-like source—or compelling signs of its presence were obtained in any wavelength, and the upper limits provided by deep observations in the various bands are often perceived as ruling out the presence of a "standard" neutron star (see, e.g., McCray 1993, 2007; Graves et al. 2005; Park et al. 2005; Manchester 2007; McCray & Fransson 2016).

The aim of this work is to appraise the situation using currently available X-ray data. We derive new upper limits on the emission from a compact source in SN 1987A from recent *Chandra* observations, trying also to take into account the uncertainties due to the complicate environment and to the unknown pulsar's spectrum and rotational parameters. We then discuss the results in the context of the properties of neutron stars. In the following, unless the precise nature of the possible compact object left in SN 1987A is the focus of a sentence, we will use neutron star, pulsar, and central source or object, more or less like synonyms.

2. The *Chandra* Observations

The *Chandra X-ray Observatory* is the only instrument with high enough spatial resolution to resolve (partially) the structure of SN 1987A in X-rays. *Chandra* has two focal plane instruments: the micro-channel plate High Resolution Camera (HRC; Murray et al. 2000) and the Advanced CCD Imaging Spectrometer (ACIS; Garmire et al. 2003). The ACIS provides somewhat lower spatial resolution than the HRC, and in imaging mode, its readout speed is inadequate to sample the period of a fast-spinning pulsar, but it has a much larger effective area, especially at high energies, and is therefore

Table 1
Log of the *Chandra* Observations Used in This Work

Instrument	Obs.ID	Date yyyy mm dd	Exposure (ks)
ACIS-S/HETG	15809	2014 Mar 13	70.5
HRC-S/LETG	16757	2015 Mar 14	67.7
ACIS-S/HETG	16756	2015 Sep 17	66.6

better suited for our purpose. In fact, the effective area of the HRC drops rapidly by a factor ∼4 after the peak at 1 keV and above 2 keV is several time smaller than that of the ACIS. As the opacity of the envelope to the high-energy emission is expected to decrease with time approximately as $\propto t^2$ (e.g., McCray 1993; Chevalier & Fransson 1994; Perna et al. 2008), here we used only the data from three of the longest and most recent *Chandra* observations in the archive (see Table 1 and Frank et al. 2016 for their details, and Park et al. 2004, 2005; Ng et al. 2009 for limits from older observations).

The data were processed and analyzed with the *Chandra* Interactive Analysis of Observations software package (CIAO version 4.8; Fruscione et al. 2006) and the calibration files in the CALDB database (version 4.7.1.). In all of the observations, the instruments were operated with the grating spectrometers, the Low Energy Transmission Grating (LETG) for the HRC and the High Energy Transmission Grating (HETG) for the ACIS. All of the analysis presented here is based on the zero-order images, count rates, and spectra. We note that the significant advantage of the ACIS over the HRC in terms of effective area for hard photons remains also when the transmission gratings are used.[8] For the ACIS data, we removed the pixel randomization added by the *Chandra* software and used the energy-dependent sub-pixel event repositioning algorithm by Li et al. (2004) to achieve sub-pixel resolution. The HRC data were used mainly to check that the procedure did not produce image artefacts.

2.1. Analysis of the ACIS Data

In the X-ray band, at the time of the observations we considered (2014–2015, see Table 1), SN 1987A could be enclosed in a ≈3″ by 4″ (axes) ellipse (see Figure 1). The innermost structure, the "equatorial ring" (radius $R \approx 0\farcs4$, equivalent to ∼0.1 pc at 50 kpc), has been interacting with the ejecta for many years (Frank et al. 2016) and is rather bright in X-rays (Figure 1).

The main aims of the analysis described in this section are to see whether there are reasons to suspect that part of the X-rays originate from a pulsar and to measure the absorption in its direction. For the two ACIS observations, we extracted the spectra from an inner circular region with radius of 0.″3 (Figure 1). This choice, which entails the use of only a small fraction of the photon collected with *Chandra*, is motivated by the fact that for reasonable assumptions on the speed of a neutron star (projected velocity $<2000\,\mathrm{km\,s^{-1}}$, see e.g., Hobbs et al. 2005), the compact source must be within this radius. The background spectra were extracted from an annulus with radii of 2″ and 4″, well outside the X-ray-bright rim of the supernova. This selection resulted in 0.5–8 keV spectra of 414 photons for the first observation (net source count rate of $(5.8 \pm 0.3) \times 10^{-3}$ counts $\mathrm{s^{-1}}$, for a total of 411 ± 20 source counts and a signal-to-noise ratio of 99.4%) and 325 photons for the second observation (net source count rate of $(4.8 \pm 0.3) \times 10^{-3}$ counts $\mathrm{s^{-1}}$, 323 ± 18 net counts and signal-to-noise of 99.3%).

The spectra can be described by a model with one or more shock components (we used pshock in XSPEC/xspshock in Sherpa) modified for the absorption. Similarly to previous analyses (e.g., Zhekov et al. 2006), we found that the fit with a one-shock model results in an unreasonably low value of the absorption column density ($\sim 9 \times 10^{19}\,\mathrm{cm^{-2}}$), consistent with zero and much lower that both the average total Galactic column density toward the LMC ($1.6 \times 10^{21}\,\mathrm{cm^{-2}}$; Kalberla et al. 2005) and the density measured in the direction of SN 1987A ($\sim(2\text{–}3) \times 10^{21}\,\mathrm{cm^{-2}}$; Fitzpatrick & Walborn 1990; Michael et al. 2002; Park et al. 2004; Kalberla et al. 2005). Additionally, fixing the $N_{\rm H}$ to a more plausible value of $2 \times 10^{21}\,\mathrm{cm^{-2}}$, we obtained a worse fit (although, still statistically acceptable), with a reduced χ^2 (χ^2_ν) that increased from 1.18 for 29 degrees of freedom (dof) to 1.43 for 30 dof. On the other hand, a two-shock model yields an absorption, as well as temperatures, in agreement with previous works. To obtain a better estimate of the magnitude of the absorption,[9] we fit simultaneously the two spectra with a numerical factor to account for the different fluxes (the results of the simultaneous fit are consistent with those of the individual fits). We obtained $N_{\rm H} = (2.6^{+0.8}_{-0.9}) \times 10^{21}\,\mathrm{cm^{-2}}$ (with the solar-system abundances by Anders & Grevesse 1989 and the photoelectric absorption cross sections by Balucinska-Church & McCammon 1992), $kT_1 = 0.7^{+0.4}_{-0.2}$ keV and $kT_2 = 2.8^{+1.5}_{-0.5}$ keV, with $\chi^2_\nu = 0.88$ for 27 dof. The observed 0.5–10 keV fluxes are $\sim 1.8 \times 10^{-12}$ and $1.6 \times 10^{-12}\,\mathrm{erg\,cm^{-2}\,s^{-1}}$ for Obs.IDs 15809 and 16756, respectively. The photon statistics of the spectra is too low to fit the elemental abundances in the region, but we verified that an acceptable fit ($\chi^2_\nu = 1.02$ for 27 dof) and essentially identical results are found using the vpshock XSPEC model with the abundances fixed at the values of Zhekov et al. (2006, Table 1), who measured shock temperatures of 0.5 and 2.7 keV. We note that the use of a single absorption component with solar abundances is an oversimplification, as at least a Galactic and an LMC component should be considered; however, here we are not interested in an absolute measurement of the column density: our purpose is to parameterize the absorption with a simple indicator that will be used in the following sections. Finally, by using in Sherpa the jdpileup pileup model by Davis (2001), we estimated in both observations a pileup fraction lower than 1%, so no attempt to correct for it was made in the following.

2.2. Upper Limits on the X-Ray Emission of a Central Point Source

To set the most conservative upper limits on the luminosity of a central source, one should assume that all of the flux observed inside the central ring is produced by the central source. However, the spectral analysis of Section 2.1, with the low absorption and the shock components, strongly suggests that most of the X-ray luminosity is produced by the shocked circumstellar matter and supernova debris and does not come

[8] See, for example, http://cxc.harvard.edu/caldb/prop_plan/pimms/.

[9] Considering the relatively large uncertainties and that the two observations were taken only 18 months apart, it seems reasonable to us to assume the same $N_{\rm H}$ value for the two spectra.

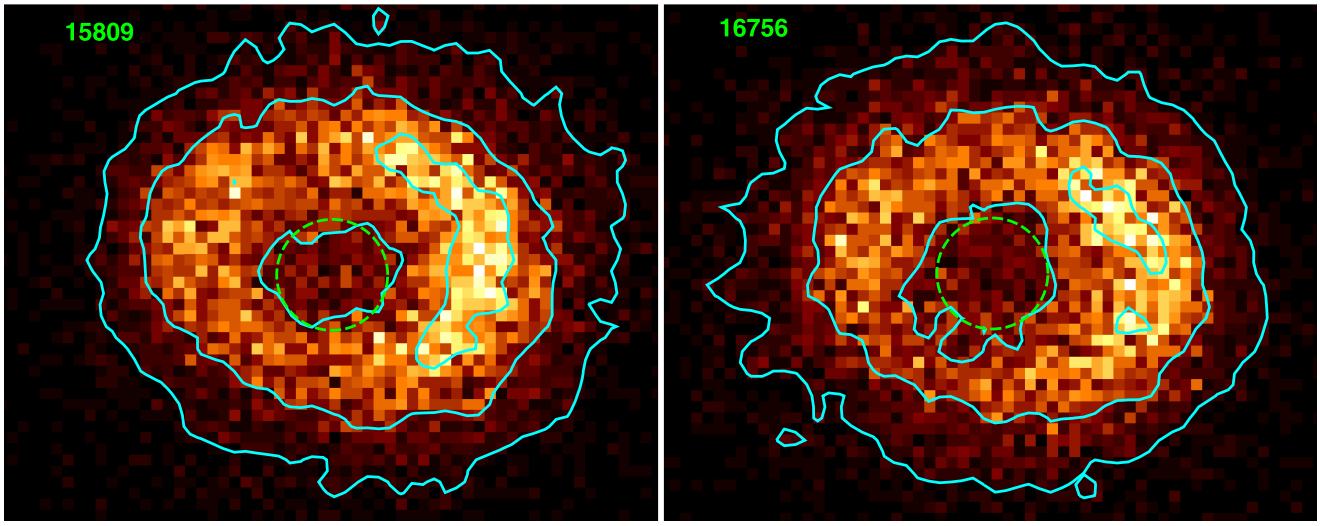

Figure 1. ACIS 2014 and 2015 images of SN 1987A in the 0.3–8 keV band with sub-pixel binning (one-eighth of the native pixel size); the Obs.ID is indicated in each panel. The dashed circles show the area we considered to evaluate the limits (approximately $0\farcs3$ radius). The brightest drawn contour levels in each panel correspond to ~25 counts bin^{-1} and the other levels are spaced by a factor of $\sqrt{2}$.

from the innermost region of the remnant, where the pulsar would be expected to reside. In light of this, we chose to estimate the upper limit as the 3σ noise level (evaluated from the Poisson fluctuations of the background) in the 0.3 arcsec radius region at the center of SN 1987A. This turned out to be 3.9×10^{-4} counts s^{-1} in observation 15809 and 4.1×10^{-4} counts s^{-1} in observation 16756 (2–8 keV), ≈30% of the 2–8 keV counts in both cases. We checked that point sources simulated with ChaRT and MARX (Carter et al. 2003; Davis et al. 2012) with those rates at the center of the supernova are detected in the X-ray images at the expected confidence level (in the simulations we adopted various thermal and nonthermal models, as well as different absorption levels, as discussed in Sections 2.2.1 and 2.2.2, but the results were virtually independent of the specific spectral shape).[10] As a further test of consistency of the different pieces of information, we fit to the 0.5–8 keV spectra a model consisting of a shock component with absorption fixed at $N_{\mathrm{H}} = 2.6 \times 10^{21}$ cm^{-2} plus a power law with photon index fixed at $\Gamma = 2.1$ (which is the model that describes the emission of the Crab pulsar in the soft X-ray band; Kirsch et al. 2005) modified by a second, independent absorption component (free to vary), so to see if the emission expected from a young pulsar is compatible with the available data. We obtained an acceptable fit and a reasonable shock temperature ($\chi^2_\nu = 1.05$ for 28 dof and $kT = (1.5 \pm 0.2)$ keV) with the "pulsar component" accounting for ≈25% of the total emission (<65% at 3σ) and a 3σ upper limit on the local absorption of $N_{\mathrm{H}} < 1.8 \times 10^{23}$ cm^{-2}.

To convert the ACIS count rate limits into luminosity limits (using XSPEC and the ancillary response files for the spectra extracted from the 0.3 arcsec radius regions to correct for the PSF and effective area fractions), several hypotheses and assumptions are necessary. We discuss them in the following sections.

Even though the bulk of the counts collected by the HRC are below 2 keV (because of the thermal spectrum and the effective area curve of the detector), for the sake of diligence, we also searched its events within 0.3 arcsec (around 1100 photons in the 0.1–10 keV band) for coherent pulsations between 0.5 ms and 1 s. No statistically significant periodic signal was found, and the upper limits on the pulsed fraction are not constraining (they are larger than 100%).

2.2.1. Thermal Emission

Let us start by considering the thermal emission that arises from the entire surface of the star due to initial cooling. For a newly born neutron star, most cooling curves indicate a surface temperature of $T_{\mathrm{eff}} \approx 2.7 \times 10^6$ K (e.g., Yakovlev & Pethick 2004; Aguilera et al. 2008; Page et al. 2009; Viganò et al. 2013), which is equivalent to $kT_{\mathrm{eff}} \approx 0.23$ keV. This value can be considered an upper limit, as the temperature would actually be lower if fast neutrino cooling processes were present (e.g., Yakovlev & Pethick 2004; Page et al. 2009). However, for prudence and to assess better the situation, we explored also the possibility of higher temperatures, up to 0.5 keV. If, for the radiating surface, we take a neutron star radius of 12 km (Lattimer 2017), the bolometric luminosity is between $L \simeq 5.5 \times 10^{34}$ and 1.2×10^{36} erg s^{-1} for $kT_{\mathrm{eff}} \approx 0.23$ and 0.5 keV, respectively.[11] The corresponding 2–8 keV unabsorbed fluxes are $\sim 3.7 \times 10^{-15}$ and 3.4×10^{-12} erg cm^{-2} s^{-1}, and the 2–8 keV X-ray luminosity for the distance $D = 53.7 \pm 3$ kpc (McCray & Fransson 2016) ranges from $L_{\mathrm{X}} \simeq 1.3 \times 10^{33}$ to 4.7×10^{35} erg s^{-1}.

A crucial issue is the absorption of the X-rays coming from the center of SN 1987A. The X-ray opacity is likely dominated by photoelectric absorption on inner-shell electrons of metals rather than by the Thomson scattering (see Corrales et al. 2016), which we shall neglect. Here, we assume the

[10] Strictly speaking, both methods yield an estimate of the sensitivity of the observation to the flux from a point source rather than an upper limit on it; however, considering the comparatively high number of photons and for the aims of this study, the two related quantities can be considered equivalent.

[11] A "color-correction" factor $f_{\mathrm{c}} = T_{\mathrm{BB}}/T_{\mathrm{eff}}$ is usually used to take into account the distortion due to the stellar atmosphere in the spectrum emitted by the neutron star surface and connect it to the observed blackbody with temperature T_{BB}. For the X-ray flux, $F_{\mathrm{X}} \propto T^4_{\mathrm{BB}}(R_{\mathrm{BB}}/D)^2 = T^4_{\mathrm{eff}}(R_\infty/D)^2$, with $R_\infty = R_{\mathrm{BB}} f_{\mathrm{c}}^2 = D_{10\ \mathrm{kpc}} \sqrt{k} f_{\mathrm{c}}^2$, where R_{BB} is the observed blackbody radius, D the distance to the source ($D_{10\ \mathrm{kpc}}$ when in units of 10 kpc), and k is the normalization of the XSPEC bbodyrad model. Typical values are in the range $1 \lesssim f_{\mathrm{c}} \lesssim 1.8$ (e.g., Özel 2013). Because the color-correction factor acts to keep the luminosity constant, correcting for the high temperatures observed, its presence would not affect our discussion.

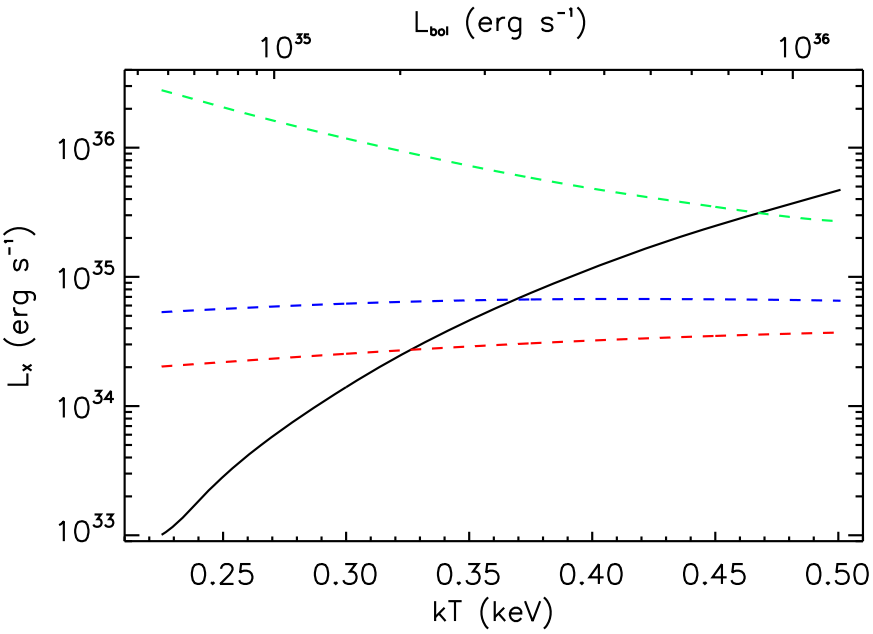

Figure 2. Constraints on the thermal emission from a neutron star. The solid black line shows the 2–8 keV X-ray luminosity as a function of the blackbody temperature (see Section 2.2.1); the upper *X*-axis show the corresponding bolometric luminosity. The dashed lines indicate the 3σ upper limits obtained for different values of $N_{\rm H}$: 3×10^{21} (red), 3×10^{22} (blue), and 1.8×10^{23} cm^{-2} (green).

envelope surrounding the compact object to be a sphere of uniform density and homogeneous composition; for the moment, for simplicity, we assume as metal abundance $Z = Z_{\odot}$, so that we can use the values derived from the spectral analysis of the inner part of the remnant, but we shall discuss this later (Section 2.2.3). We also neglect the possible ionization of the neutral matter by the central source. As the absolute minimum of the absorbing column, we posit the value derived from our X-ray fit, 2.6×10^{21} cm^{-2}, which in the following, we round off to 3×10^{21} cm^{-2}; lacking more information, for the maximum we take the above-mentioned limit of 1.8×10^{23} cm^{-2}. To have a rough order-of-magnitude reference value between these two extremes, we follow Zanardo et al. (2014), who assume the presence of $M_{\rm H} \approx 2.5\ M_{\odot}$ of matter within a region $r \simeq 0\farcs4$ (about 0.1 pc), which is roughly the size of the equatorial ring (see also Blinnikov et al. 2000; Fransson et al. 2013). Correspondingly, the density is 4×10^{-20} g cm^{-3} and $N_{\rm H} \approx 3M_{\rm H}/(4\pi m_{\rm p} r^2) \simeq 3 \times 10^{22}$ cm^{-2}, where $m_{\rm p}$ is the proton mass.[12] The corresponding limits on the thermal emission for the different absorption levels are shown in Figure 2. It is apparent that for the lower end of the range of temperatures considered ($kT \lesssim 0.3$ keV), a purely thermally emitting neutron star, even if present, would not have been detected even for the lowest conceivable $N_{\rm H}$ value.

2.2.2. Nonthermal Emission

Unless some mechanism suppressing the neutron star magnetospheric activity that converts a fraction of rotational energy into X-rays is at work, the high-energy emission of an isolated young pulsar is expected to have a large—likely dominating—contribution from a nonthermal component (e.g., Kaspi et al. 2006). For the pulsars for which the main rotational parameters (period P and slow-down rate $\dot{P}$) and the X-ray luminosity have been measured, there appears to exist a correlation between the latter quantity and the rotational energy loss $\dot{E}_{\rm rot}$ (Seward & Wang 1988; Becker & Truemper 1997). Albeit they have all a large scatter, several empirical $L_{\rm X}$–$\dot{E}_{\rm rot}$ relations have been derived from different surveys, samples of sources, etc. (see Shibata et al. 2016 and references therein); here, we adopt that of Possenti et al. (2002), $\log L_{\rm X} = 1.34 \log \dot{E}_{\rm rot} - 15.34$, which is valid over the 2–10 keV range. Under the usual assumption of a magnetic dipole rotating in vacuum, $\dot{E}_{\rm rot} = B^2 \sin^2\theta \Omega^4 R^6/(6c^3) \simeq 3 \times 10^{43} B_{14}^2 P_{10\,{\rm ms}}^{-4}$ erg s^{-1}, where $\Omega = 2\pi/P$, $P_{10\,{\rm ms}}$ is in units of 10 ms, $R = 12$ km, and for the angle between the magnetic and spin axes, we take $\theta = \pi/2$. For the spectral model, the natural choice is to use a power law with photon index fixed at $\Gamma = 2.1$, the value measured for the pulsar in the Crab Nebula (PSR J0534 +2200; $L_{\rm X} = 1.1 \times 10^{37}$ erg s^{-1}), which is the best studied young pulsar we currently know of (but note that essentially all the young rotationally powered pulsars known have similar spectral shape and slope; e.g., Becker & Truemper 1997; Possenti et al. 2002; Gotthelf 2003).

In Figure 3, we show the limits for the same $N_{\rm H}$ values discussed for the thermal emission, together with the nonthermal X-ray luminosity expected for some combinations of the neutron star period and magnetic field. While a pulsar akin to that in the Crab Nebula is not compatible with the data, there is ample room for viable combinations of parameters (e.g., $B = 10^{12}$ G and any period $P > 25$ ms).

2.2.3. The Shielding Curtain

Now we devote some attention to the composition of the matter in the curtain screening the site of the possible compact object, where metals that have a large cross section for photoelectric absorption for photons with energy of $\gtrsim$1 keV, such as C, O, Si, and Fe (Morrison & McCammon 1983), can be expected to be overabundant. We used the ejecta composition in Table 1 of Dessart & Hillier (2010), which is

[12] In principle, one should add to this value the Galactic absorption of $\sim(2–3) \times 10^{21}$ cm^{-2}. However, given the considerable uncertainties in the estimate and the relatively small size of the change, the correction is unimportant.

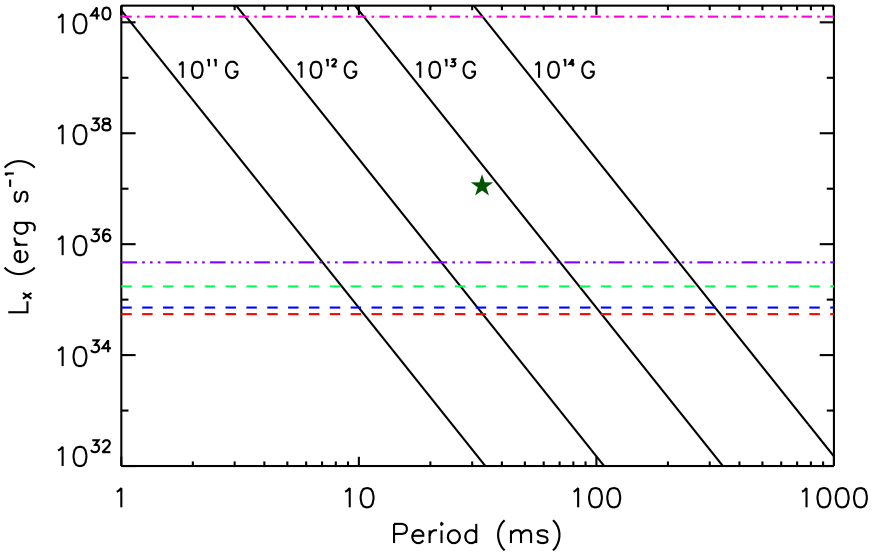

Figure 3. Constraints on the nonthermal emission from a neutron star. The solid black lines show the 2–8 keV X-ray luminosity as a function of the period for a few values of the magnetic field, as indicated by the labels. The dark green star marks the position of the Crab pulsar. The dashed lines indicate the 3σ upper limits obtained for different values of $N_{\rm H}$: 3×10^{21} (red), 3×10^{22} (blue), and 1.8×10^{23} cm^{-2} (green). The three-dotted–dashed line (violet) shows the extrapolation of the 2σ upper limit derived with *INTEGRAL* in the 20–60 keV band. The purple dotted–dashed line indicates the limit derived for the absorption with abundances similar to those of the ejecta (see Section 2.2.3).

based on hydrodynamical models by Woosley et al. (2002, and references therein), to create an abundance table for the photoelectric absorption model in XSPEC (Table 2). For the elements for which they do not provide information, we fixed the abundance at the solar value by Anders & Grevesse (1989). We stress that this is not an attempt to properly model the absorption but only to get an idea of how a non-standard composition can impact the limits.

Using the chemical mix in Table 2, the $N_{\rm H}$ of 3×10^{22} cm^{-2} that we derived from the assumption of a local density of 4×10^{-20} g cm^{-3} becomes $\approx 7.6 \times 10^{21}$ cm^{-2}. Note that the lower nominal $N_{\rm H}$ value only reflects the smaller H fraction in the mix and, with the abundances in Table 2, it actually results in a much larger X-ray abatement. In fact, with this absorption (again, we neglected the Galactic absorption component), the upper limit on the nonthermal luminosity of a pulsar derived from the data is $\approx 1.3 \times 10^{40}$ erg s^{-1} (Figure 3), which is much larger than the luminosity of the Crab pulsar. The upper limit on the thermal component is even less binding ($L_{\rm X} > 10^{41}$ erg s^{-1}).

3. Discussion and Conclusions

The mass of Sk −69° 202 and the burst of neutrinos that accompanied the explosion suggest that a neutron star was formed in SN 1987A by the process of core collapse (although it cannot be excluded that it further collapsed in a black hole if enough fallback material piled upon its surface; e.g., Zampieri et al. 1998). However, 30 years after the explosion and despite observations in every band of the electromagnetic spectrum, there is still no positive evidence for a compact object of any kind in the remnant.

Optical and ultraviolet (UV) searches were performed for both periodic signals and point-like emission. After some claims of detection of pulsations that were later retracted or not confirmed by subsequent observations or reanalysis, upper limits on the pulsed emission for periods between 0.2 and 10 s were set with a limiting V magnitude of ∼24.6 using *HST* and the ground-based Anglo-Australian Telescope (Percival et al. 1995; Manchester & Peterson 1996). Graves et al. (2005) assumed an attenuation due to the dust absorption in the

Table 2
Abundances Adopted

Element	Solar System Z/H	Custom Z/H
H	1.00	1.00
He	9.77e–02	2.29
Li	1.45e–11	1.45e–11
Be	1.41e–11	1.41e–11
B	3.98e–10	3.98e–10
C	3.63e–04	1.55e–01
N	1.12e–04	6.85e–03
O	8.51e–04	3.05e–01
F	3.63e–08	3.63e–08
Ne	1.23e–04	8.63e–02
Na	2.14e–06	2.14e–06
Mg	3.80e–05	1.52e–02
Al	2.95e–06	2.95e–06
Si	3.55e–05	2.03e–02
P	2.82e–07	2.82e–07
S	1.62e–05	7.61e–03
Cl	3.16e–07	3.16e–07
Ar	3.63e–06	1.27e–03
K	1.32e–07	1.32e–07
Ca	2.29e–06	1.02e–03
Sc	1.26e–09	1.26e–09
Ti	9.77e–08	1.65e–05
V	1.00e–08	1.00e–08
Cr	4.68e–07	4.68e–07
Mn	2.45e–07	2.45e–07
Fe	4.68e–05	2.54e–03
Co	8.32e–08	8.32e–08
Ni	1.78e–06	2.13e–02
Cu	1.62e–08	1.62e–08
Zn	3.98e–08	3.98e–08

Note. The solar system values are from Anders & Grevesse (1989) and all abundances are relative to H.

remnant $\leqslant$97% and derived with *HST* UV/optical limits on the luminosity of a compact remnant of a few $\times 10^{33}$ to 10^{34} erg s^{-1}. Recent observations in the far-infrared (IR) and in the sub-mm continuum with *Herschel* and ALMA (Matsuura et al. 2011, 2015; Indebetouw et al. 2014) showed the presence of substantial amount of dust in the ejecta. If the dust is distributed in clumps, some light could scatter around the clumps, and the extinction could be lower than the limit assumed by Graves et al. (2005), at least in some lines of sight. However, if nearly half a solar mass of dust (Matsuura et al. 2011, 2015; Indebetouw et al. 2014) fills the ejecta uniformly, even higher extinction might be possible and the site of the pulsar would be cloaked in a cloud impenetrable to the IR/optical light.

A limit on the luminosity of the alleged central source can also be derived by comparing the bolometric emission of the remnant with the power injected by titanium-44 (^{44}Ti) decay (Grebenev et al. 2012; Boggs et al. 2015; McCray & Fransson 2016). The decay of the ^{44}Ti at 10000 days is expected to deposit energy at a rate of $L_{^{44}\mathrm{Ti}} \sim 280\ L_{\odot}$, most of which is radiated at IR wavelengths from a population of $\sim 0.5\ M_{\odot}$ of dust grains (Matsuura et al. 2011; Indebetouw et al. 2014) with luminosity $L_{\mathrm{dust}} \sim 220\ L_{\odot}$. While there seems not to be much room for an additional energy input from a central source, one must consider that (i) both the ^{44}Ti energy deposition and the IR luminosity have uncertainties of the order of 20% or more and (ii) most of the X-ray flux from the central source would be absorbed via photoionization, the majority of the energy (≈75%) being used to photoionize and only the remaining (≈25%) available for heating of the dust particles.[13] We conclude that the comparison of the dust emission with the ^{44}Ti energy deposition rates is consistent with the presence of a central source with a luminosity of $L_{\mathrm{dust}} - fL_{^{44}\mathrm{Ti}} \gtrsim 100\ L_{\odot}$ ($\sim 4 \times 10^{35}$ erg s^{-1}).

Repeated observations in radio at different frequencies provided limits on the flux density $<115\ \mu$Jy for pulsed emission (Manchester 2007). These limits are not particularly constraining, however, because of the large distance to the LMC (e.g., Manchester et al. 2005). Furthermore, the non-detection could be due to free–free absorption in the supernova remnant (see also Wang et al. 2017) or simply to an unfavorable beaming. Indeed, there are numerous young and energetic pulsars (including and, seemingly, mostly rotation-powered ones) that are not detected as radio pulsars (e.g., Caraveo 2014).

In X-rays, the deepest upper limits on the emission of a point source can be obtained using *Chandra*. We believe that, when the substantial uncertainties involved in the X-ray analysis (in particular, in the absorption) are considered, the limits are not particularly restrictive even in this band. The thermal component of the emission of a pulsar would easily escape detection in the available data sets; in particular, for the lower temperatures in the range of what can be expected from a "baby" neutron star ($kT \lesssim 0.3$ keV), the limits are not constraining even in the case of the lowest conceivable absorption, corresponding to the total Galactic N_{H} (with solar-system abundances) along the line of sight toward SN 1987A (Figure 2).

In the case of the nonthermal emission, the situation is more critically dependent on the absorption. A pulsar as bright in X-rays as the one in the Crab Nebula (and with a similar emission spectrum) should be detectable for the range of N_{H} that we explored if the composition of the absorbing matter is similar to that of the solar system. However, our exercise of altering the chemical composition of the absorber, so to reflect an enrichment of the elements that should be abundant in the ejecta of a massive star at the end of its life, shows that the X-ray limits become totally loose in the instance of very high metallicity. In that case, the Crab pulsar itself could be lurking in the remnant (Section 2.2.3). Lacking sound information on the quantity and the composition (and ionization state) of the absorbing gas, the most reliable limits are probably those obtained in soft γ-rays. Using the IBIS/ISGRI hard-X-ray telescope on board *INTEGRAL*, Grebenev et al. (2012) derived a 2σ upper limit of 3×10^{35} erg s^{-1} in the 20–60 keV band for a power-law continuum with photon index $\Gamma = 2.1$. This value, extrapolated to the 2–8 keV band by assuming the Crab pulsar's spectrum, corresponds to 4.7×10^{35} erg s^{-1}, as shown in Figure 3. This luminosity is higher than, but comparable to, the limits that we obtained assuming solar-system-like abundances: a few $\times 10^{35}$ erg s^{-1} (Figure 3). It is also consistent with the limit derived from the reprocessed radiation from the ^{44}Ti decay. We note that for a pulsar, a nonthermal X-ray luminosity of ≈(1–5) $\times 10^{35}$ erg s^{-1} corresponds to a rotational energy loss of ≈(0.5–1.5) $\times 10^{38}$ erg s^{-1}.

Overall, it seems that while a Crab-like pulsar is incompatible with the observations (essentially, the γ-ray observations), there is ample room for the presence of an X-ray-emitting neutron star. In fact, many combinations of period and magnetic field plausible for an ordinary young neutron star are allowed by the limits in Figure 3. A recent work by Gullón et al. (2014), for instance, found that the observed Galactic population of neutron stars is well reproduced by distributions of initial periods (P_0) in the range 0.1–0.5 s, with only a small fraction of objects with $P_0 < 0.1$ s, and initial magnetic field strength $\log B_0[\mathrm{G}] \approx 13.0$–$13.2$ with width $\sigma(\log B_0) = 0.6$–0.7 (see also Faucher-Giguère and Kaspi 2006; Popov et al. 2010).

While a supposed pulsar in SN 1987A does not necessarily have to be an "unusual" neutron star, an object similar to the so-called "central compact objects" (CCOs; e.g., De Luca 2017) is certainly a very viable possibility. CCOs are steady X-ray sources with seemingly thermal spectra and no counterparts in radio and gamma wavebands; their periods, although measured in only a few sources, are in the 0.1–0.5 s range. These properties are clearly consistent with the observational constraints for SN 1987A, and CCOs seem to be relatively common in our Galaxy (De Luca et al. 2008). The emerging scenario for CCOs is that of young neutron stars either born with a weak magnetic field ($B < 10^{11}$ G) or with a normal field "buried" beneath the surface (Ho 2011; Viganò & Pons 2012; Gotthelf et al. 2013). In the latter hypothesis, the submergence of the magnetic field is the consequence of a stage of hypercritical accretion of debris matter after the supernova explosion, a situation that could have taken place in SN 1987A (Viganò & Pons 2012). Conversely, a magnetar, given their

[13] We considered a power-law photon spectrum with index α, $\frac{dn}{d\nu} = N_0\left(\frac{\nu}{\nu_0}\right)^{-\alpha}$, and we approximated the photoionization cross section as $\sigma(\nu) = \sigma_0\left(\frac{\nu}{\nu_0}\right)^{-3}$. The ratio of the energy in heat over the total photoionization energy is $f = \frac{E_{\mathrm{thermal}}}{E_{\mathrm{total}}} = \frac{\int_{\nu_0}^{+\infty}(h\nu - h\nu_0)\sigma(\nu)\frac{dn}{d\nu}d\nu}{\int_{\nu_0}^{+\infty}h\nu\sigma(\nu)\frac{dn}{d\nu}d\nu} = \frac{1}{\alpha+2}$. For $\alpha = 0$, half of the energy goes into heating. For a more reasonable $\alpha = 2$, only 25% of the absorbed radiation is turned into heat.

typically higher thermal luminosities and hotter thermal components with respect to normal neutron stars (Perna et al. 2013; Viganò et al. 2013), would be somewhat disfavored.

Finally, a new interesting piece of information has been recently produced by Zanardo et al. (2014), who reported on the possible detection with ALMA at 102–672 GHz (after removing synchrotron emission modeled with ATCA at 44 GHz) of a flat-spectrum region slightly westward of the SN site, whose properties are consistent with a pulsar wind nebula (PWN). They estimated $L_{\rm PWN} \approx 5.4 \times 10^{33}$ erg s^{-1} for frequencies between 102 and 672 GHz. If the PWN is powered by the pulsar with an efficiency of ∼1%, the radio luminosity implies a rotational energy loss $\dot{E}_{\rm rot} \lesssim 10^{35}$ erg s^{-1} and hence an X-ray luminosity not larger than $L_{\rm X} \approx 10^{32}$ erg s^{-1} (Zanardo et al. 2014). Even in the case that the identification of the PWN is correct, we do not regard these limits as compelling, considering that the luminosity in the 102–672 GHz would be only a lower limit for its emission. Furthermore, the relationship between pulsar spin-down power and PWN luminosity is rather uncertain and, similarly to the $L_{\rm X}$–$\dot{E}_{\rm rot}$ relation for pulsars, has a large scattering (e.g., Mattana et al. 2009). However, this candidate PWN is the only hint of the presence of a pulsar in SN 1987A obtained so far. Further studies of this possible PWN or, more in general, the detection of a compact radio source with flat spectrum and/or polarized emission near the center of the supernova remnant probably represent the best hope to establish the presence of a neutron star in SN 1987A in the next few years.

This research is based on observations made by the *Chandra X-ray Observatory* and has made use of software provided by the *Chandra* X-ray Center (CXC) in the application packages CIAO, ChIPS, and Sherpa. P.E. and N.R. acknowledge funding in the framework of the NWO Vidi award A.2320.0076. M.M. is supported by an STFC Ernest Rutherford fellowship (ST/L003597/1). R.P. was partly supported by NSF award AST-1616157. We thank the anonymous referee for many valuable comments. P.E. is grateful to Lia Corrales, Sandro Mereghetti, Elisa Costantini, and Mathieu Renzo for useful discussions. R.P. and P.E. are grateful to Richard McCray for relevant information.

Facility: Chandra (ACIS, HRC).

Software: ChaRT (Carter et al. 2003), CIAO (v4.8; Fruscione et al. 2006), FTOOLS (v6.21; Blackburn et al. 1995), MARX (v5.3; Davis et al. 2012), Sherpa (Freeman et al. 2001), XSPEC (v12.9.1; Arnaud et al. 1996).

ORCID iDs

Paolo Esposito https://orcid.org/0000-0003-4849-5092
Nanda Rea https://orcid.org/0000-0003-2177-6388
Davide Lazzati https://orcid.org/0000-0002-9190-662X
Mikako Matsuura https://orcid.org/0000-0002-5529-5593
Rosalba Perna https://orcid.org/0000-0002-3635-5677
José A. Pons https://orcid.org/0000-0003-1018-8126

References

Aguilera, D. N., Pons, J. A., & Miralles, J. A. 2008, A&A, 486, 255
Alekseev, E. N., Alekseeva, L. N., Volchenko, V. I., & Krivosheina, I. V. 1987, JETPL, 45, 589
Anders, E., & Grevesse, N. 1989, GeCoA, 53, 197
Arnaud, K. A. 1996, in ASP Conf. Ser. 101, Astronomical Data Analysis Software and Systems V, ed. G. H. Jacoby & J. Barnes (San Francisco, CA: ASP), 17
Arnett, W. D., Bahcall, J. N., Kirshner, R. P., & Woosley, S. E. 1989, ARA&A, 27, 629
Balucinska-Church, M., & McCammon, D. 1992, ApJ, 400, 699
Becker, W., & Truemper, J. 1997, A&A, 326, 682
Bionta, R. M., Blewitt, G., Bratton, C. B., Casper, D., & Ciocio, A. 1987, PhRvL, 58, 1494
Blackburn, J. K. 1995, in ASP Conf. Ser. 77, Astronomical Data Analysis Software and Systems IV, ed. R. A. Shaw, H. E. Payne, & J. J. E. Hayes (San Francisco, CA: ASP), 367
Blinnikov, S., Lundqvist, P., Bartunov, O., Nomoto, K., & Iwamoto, K. 2000, ApJ, 532, 1132
Blum, K., & Kushnir, D. 2016, ApJ, 828, 31
Boggs, S. E., Harrison, F. A., Miyasaka, H., et al. 2015, Sci, 348, 670
Caraveo, P. A. 2014, ARA&A, 52, 211
Carter, C., Karovska, M., Jerius, D., Glotfelty, K., & Beikman, S. 2003, in ASP Conf. Ser. 295, Astronomical Data Analysis Software and Systems XII, ed. H. E. Payne, R. I. Jedrzejewski, & R. N. Hook San. Francisco (San Francisco, CA: ASP), 477
Chevalier, R. A., & Fransson, C. 1994, ApJ, 420, 268
Chita, S. M., Langer, N., van Marle, A. J., García-Segura, G., & Heger, A. 2008, A&A, 488, L37
Corrales, L. R., García, J., Wilms, J., & Baganoff, F. 2016, MNRAS, 458, 1345
Davis, J. E. 2001, ApJ, 562, 575
Davis, J. E., Bautz, M. W., Dewey, D., et al. 2012, Proc. SPIE, 8443, 84431A
De Luca, A. 2008, in AIP Conf. Proc. 983, 40 years of Pulsars: Millisecond Pulsars, Magnetars and More, ed. C. Bassa et al. (Melville, NY: AIP), 311
De Luca, A. 2017, JPhCS, 932, 021006
Dessart, L., & Hillier, D. J. 2010, MNRAS, 405, 2141
Faucher-Giguère, C.-A., & Kaspi, V. M. 2006, ApJ, 643, 332
Fitzpatrick, E. L., & Walborn, N. R. 1990, AJ, 99, 1483
Frank, K. A., Zhekov, S. A., Park, S., et al. 2016, ApJ, 829, 40
Fransson, C., Larsson, J., Spyromilio, J., et al. 2013, ApJ, 768, 88
Freeman, P., Doe, S., & Siemiginowska, A. 2001, Proc. SPIE, 4477, 76
Fruscione, A., McDowell, J. C., Allen, G. E., et al. 2006, Proc. SPIE, 6270, 62701V
Garmire, G. P., Bautz, M. W., Ford, P. G., Nousek, J. A., & Ricker, G. R., Jr. 2003, Proc. SPIE, 4851, 28
Gilmozzi, R., Cassatella, A., Clavel, J., et al. 1987, Natur, 328, 318
Gotthelf, E. V. 2003, ApJ, 591, 361
Gotthelf, E. V., Halpern, J. P., & Alford, J. 2013, ApJ, 765, 58
Graves, G. J. M., Challis, P. M., Chevalier, R. A., et al. 2005, ApJ, 629, 944
Grebenev, S. A., Lutovinov, A. A., Tsygankov, S. S., & Winkler, C. 2012, Natur, 490, 373
Gullón, M., Miralles, J. A., Viganò, D., & Pons, J. A. 2014, MNRAS, 443, 1891
Hillebrandt, W., Hoeflich, P., Weiss, A., & Truran, J. W. 1987, Natur, 327, 597
Hirata, K., Kajita, T., Koshiba, M., Nakahata, M., & Oyama, Y. 1987, PhRvL, 58, 1490
Ho, W. C. G. 2011, MNRAS, 414, 2567
Hobbs, G., Lorimer, D. R., Lyne, A. G., & Kramer, M. 2005, MNRAS, 360, 974
Indebetouw, R., Matsuura, M., Dwek, E., et al. 2014, ApJL, 782, L2
Kalberla, P. M. W., Burton, W. B., Hartmann, D., et al. 2005, A&A, 440, 775
Kaspi, V. M., Roberts, M. S. E., & Harding, A. K. 2006, in Compact Stellar X-ray Sources, ed. W. H. G. Levin & M. van der Klis (Cambridge: Cambridge Univ. Press), 279
Kirsch, M. G., Briel, U. G., Burrows, D., et al. 2005, Proc. SPIE, 5898, 22
Lattimer, J. M. 2017, IJMPE, 26, 1740014
Li, J., Kastner, J. H., Prigozhin, G. Y., et al. 2004, ApJ, 610, 1204
Manchester, R. N. 2007, in AIP Conf. Ser. 937, Supernova 1987A: 20 Years After: Supernovae and Gamma-Ray Bursters, ed. S. Immler, K. Weiler, & R. McCray (Melville, NY: AIP), 134
Manchester, R. N., Hobbs, G. B., Teoh, A., & Hobbs, M. 2005, AJ, 129, 1993
Manchester, R. N., & Peterson, B. A. 1996, ApJL, 456, L107
Matsuura, M., Dwek, E., Barlow, M. J., et al. 2015, ApJ, 800, 50
Matsuura, M., Dwek, E., Meixner, M., et al. 2011, Sci, 333, 1258
Mattana, F., Falanga, M., Götz, D., et al. 2009, ApJ, 694, 12
McCray, R. 1993, ARA&A, 31, 175
McCray, R. 2007, in AIP Conf. Ser. 937, Supernova 1987A: 20 Years After: Supernovae and Gamma-Ray Bursters, ed. S. Immler, K. Weiler, & R. McCray (Melville, NY: AIP), 3
McCray, R., & Fransson, C. 2016, ARA&A, 54, 19
Michael, E., Zhekov, S., McCray, R., et al. 2002, ApJ, 574, 166

Morris, T., & Podsiadlowski, P. 2007, Sci, 315, 1103
Morrison, R., & McCammon, D. 1983, ApJ, 270, 119
Murray, S. S., Austin, G. K., Chappell, J. H., et al. 2000, Proc. SPIE, 4012, 68
Ng, C.-Y., Gaensler, B. M., Murray, S. S., et al. 2009, ApJL, 706, L100
Özel, F. 2013, RPPh, 76, 016901
Page, D., Lattimer, J. M., Prakash, M., & Steiner, A. W. 2009, ApJ, 707, 1131
Park, S., Zhekov, S. A., Burrows, D. N., Garmire, G. P., & McCray, D. 2005, AdSpR, 35, 991
Park, S., Zhekov, S. A., Burrows, D. N., Garmire, G. P., & McCray, R. 2004, ApJ, 610, 275
Percival, J. W., Boyd, P. T., Biggs, J. D., et al. 1995, ApJ, 446, 832
Perego, A., Hempel, M., Fröhlich, C., et al. 2015, ApJ, 806, 275
Perna, R., Soria, R., Pooley, D., & Stella, L. 2008, MNRAS, 384, 1638
Perna, R., Viganò, D., Pons, J. A., & Rea, N. 2013, MNRAS, 434, 2362
Podsiadlowski, P. 1992, PASP, 104, 717
Popov, S. B., Pons, J. A., Miralles, J. A., Boldin, P. A., & Posselt, B. 2010, MNRAS, 401, 2675
Possenti, A., Cerutti, R., Colpi, M., & Mereghetti, S. 2002, A&A, 387, 993
Rousseau, J., Martin, N., Prévot, L., et al. 1978, A&AS, 31, 243
Seward, F. D., & Wang, Z.-R. 1988, ApJ, 332, 199
Shibata, S., Watanabe, E., Yatsu, Y., Enoto, T., & Bamba, A. 2016, ApJ, 833, 59
Sonneborn, G., Altner, B., & Kirshner, R. P. 1987, ApJL, 323, L35
Viganò, D., & Pons, J. A. 2012, MNRAS, 425, 2487
Viganò, D., Rea, N., Pons, J. A., et al. 2013, MNRAS, 434, 123
Walborn, N. R., Prevot, M. L., Prevot, L., et al. 1989, A&A, 219, 229
Wang, S.-Q., Wang, N., Wang, D.-H., & Shang, L.-H. 2017, ChPhL, 34, 129702
Woosley, S. E., Heger, A., & Weaver, T. A. 2002, RvMP, 74, 1015
Woosley, S. E., Pinto, P. A., Martin, P. G., & Weaver, T. A. 1987, ApJ, 318, 664
Yakovlev, D. G., & Pethick, C. J. 2004, ARA&A, 42, 169
Zampieri, L., Colpi, M., Shapiro, S. L., & Wasserman, I. 1998, ApJ, 505, 876
Zanardo, G., Staveley-Smith, L., Indebetouw, R., et al. 2014, ApJ, 796, 82
Zhekov, S. A., McCray, R., Borkowski, K. J., Burrows, D. N., & Park, S. 2006, ApJ, 645, 293